The Analytic Way to the Red Giant Branch

I. Saviane [1]
and A. Rosenberg [2]

[1]Dipartimento di Astronomia, Università di Padova
[2]Instituto de Astrofísica de Canarias

Abstract: A recent analysis of the Rosenberg et al. (1999a, A&A, in press; 1999b, A&A, submitted) database, has yielded new calibrations of a full set of metallicity indices. The homogenous material has also allowed us to define an analytic function that is able to reproduce the observed morphology of the Galactic globular cluster red giant branch (Saviane et al. 1999, A&A, in press). We outline here the basic methodology and the results that were obtained, and present some test cases that represent possible applications of these new calibration data.

1 Introduction

It is a well established observational fact that the morphology and location, in the color-magnitude diagram (CMD), of the red giant branch (RGB) of Galactic globular clusters (GGCs) depend on the metallicity of the cluster (Sandage & Wallerstein 1960; Sandage & Smith 1966). This property has been used in the past to devise several metallicity indices, which are used to estimate [Fe/H] for those clusters that lack direct spectroscopic measurements.

The RGB is also an intrisically bright feature in the V and I bands (up to $M_I \simeq -4$ and $M_I \simeq -3$), so it can be used for a first estimate of the metallicity of the old populations in distant galaxies. Limiting magnitudes of the order $V = 25$ can be reached with current ground based instrumentation, and $V = 26$ with HST or VLT, which means that the brightest RGB stars can be resolved out to distance moduli $m-M \simeq 30$. Actually, useful metallicity estimates can be obtained if at least 1 mag is covered along the RGB, so this method is used for galaxies inside and close to the Local Group.

The common procedure is to compare the observed RGB to the standard branches of Da Costa & Armandroff (1990; DA90), either directly (e.g. Saviane, Held & Piotto 1996) or making use of the interpolation formulae provided by DA90 and Lee, Freedman & Madore (1993; LFM93). The mean color of the RGB, measured at some conventional absolute magnitude, is then converted into a mean metallicity.

Although the DA90 RGBs are still the conventional reference for metallicity determinations within the Local Group (LG), new observational data have accumulated in recent years, that allow us to further refine our methods. In particular, we now have (a) a new metallicity scale based on a homogenous high-resolution spectroscopic database and analysis of 24 globulars (Carretta & Gratton 1997, GC97); (b) a calibration of the CaII infrared triplet equivalent widths

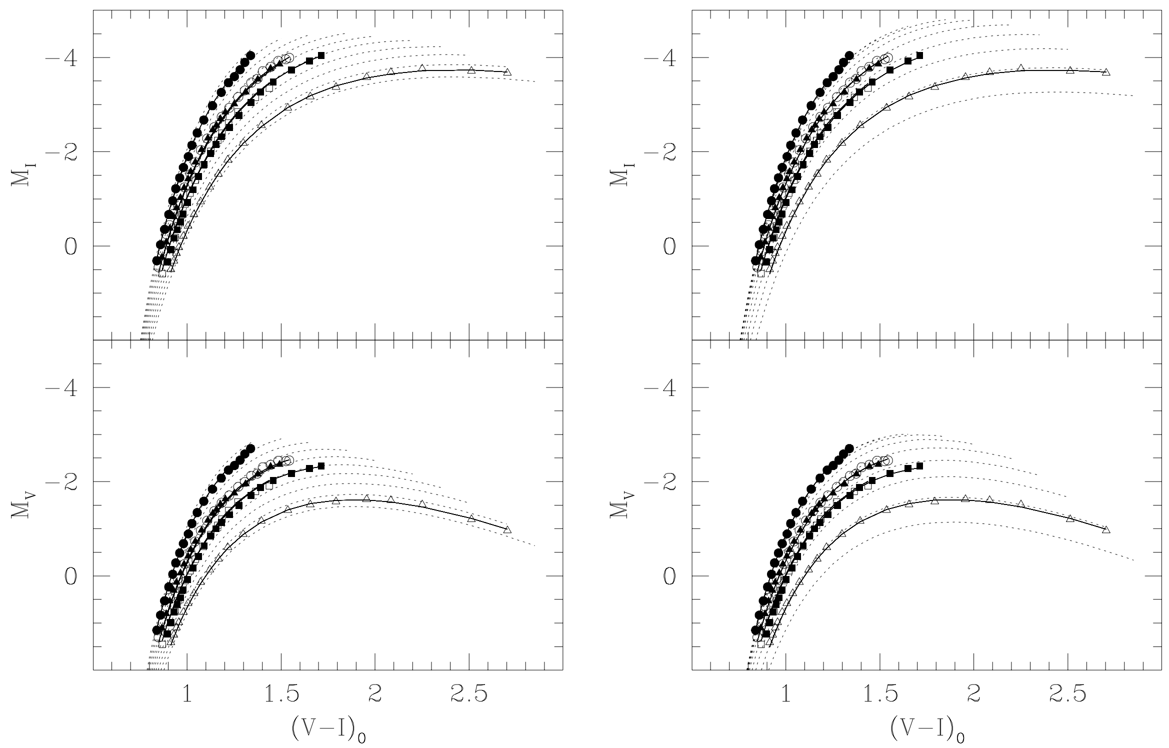

Figure 1: Results of the fits, both on the ZW84 metallicity scale (left panel) and that of GC97 (right panel). The Lee, Demarque & Zinn (1990) distance scale is adopted

for 71 GGCs both on the CG97 and the Zinn & West (1984; ZW84) metallicity scales (Rutledge, Hesser & Stetson 1997; RHS97); and (c) two homogeneous CCD photometric databases of GGCs. These are the groundbased V, I photometry of 52 clusters presented in Rosenberg et al. (1999a,b) and the B, V photometry of 20 clusters presented in Piotto et al. (1997), where each cluster is covered from a few mag below the turnoff up to the RGB tip.

The first large scale study based on these internally self-consistent photometric and spectroscopic data sets has been the relative-age investigation of GGCs carried out in Rosenberg et al. (1999c), where the advantages of using homogeneous data sets were shown.

As a second step, we began a new study to calibrate a complete set of metallicity indices on the ZW84 and CG97 scales, and to obtain an analytic description of the RGB morphology as a function of metallicity. The final goal is to improve the mean [Fe/H] determinations of populations II within the Local Group, extending the methods of LFM93. And, more important, *metallicity distributions* will also be obtained in a more direct way.

The new analysis of the groundbased data is now complete (Saviane et al. 1999), and a companion study of the HST material is being carried out. With this contribution, we want to briefly outline the method that was followed, and to suggest possible applications of our RGB description. The readers are referred to the main paper for any futher detailes. We also stress here that, when talking about the Zinn & West or Carretta & Gratton metallicity scales, we will actually mean the RHS97 equivalent widths calibrated onto the two scales.

2 RGB Morphology vs. Metallicity

It was noticed during the relative age investigation, that a hyperbolic function of the form

$$M_I = a + b \cdot (V - I) + c/[(V - I) - d] \quad (1)$$

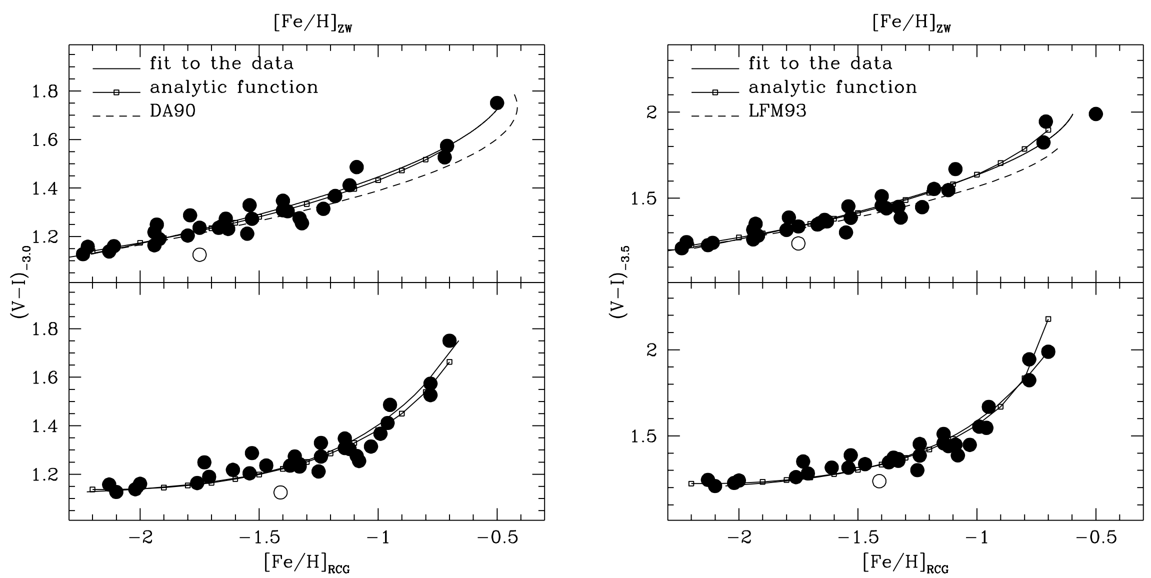

Figure 2: The observed trends of the indices $(V-I)_{-3.0}$ and $(V-I)_{-3.5}$ with metallicity. The solid line represents the fit to the data, whereas the trend predicted by the analytic function is represented by open squares connected with a solid line. The CG97 metallicity scale is used in the lower panels, and that of ZW84 in the upper panels. In the upper panels, the dashed lines represent the calibrations of Da Costa & Armandroff (1990) and Lee, Freedman & Madore (1993)

is a good approximation to the RGB, in particular since it can reproduce the branches of even the metal richest clusters. It was then guessed that it could be possible to reproduce any RGB by writing a, b, c and d as functions of the metallicity, provided that a distance scale is assumed.

For this purpose, a subset of clusters was selected from the Rosenberg et al. database, in order to define a fixed RGB grid, and to constrain the four parameters. The clusters had to have a significant number of stars on the RGB, a low reddening ($E_{B-V} \leq 0.05$) and, taken together, to cover a wide metallicity range ($-2.2 \leq$ [Fe/H]$_{\rm ZW} \leq -0.7$). Six clusters satisfy these criteria, namely NGC 104 (47 Tuc), NGC 288, NGC 5272 (M3), NGC 5904 (M5), NGC 6205 (M13) and NGC 6341 (M92).

The fiducial RGBs were then extracted from the CMDs, and they were converted to the absolute $M_I, (V-I)_0$ plane, assuming that $E_{V-I} = 1.28 \times E_{B-V}$ (Dean, Warren & Cousins 1978), and that $M_V^{\rm HB} = a \times$[Fe/H]$+b$. The apparent HB magnitudes were taken from Rosenberg et al. (1999c). Afterwards, Eq. (1) was fitted to the data, assuming that each coefficient is a quadratic function of [Fe/H], of the form $a = k_1$[Fe/H]$^2 + k_2$[Fe/H]$+ k_3$, etc. Moreover, we found that d has only small variations with metallicity, so we kept $d = const$.

The fits were obtained for all combinations of two distance and two metallicity scales. Both the CG97 and ZW84 metallicity scales were used, and, with respect to the HB absolute magnitude, we used both the Lee, Demarque & Zinn (1990; LDZ) scale (M_V(HB) $= 0.17 \times$ [Fe/H] $+ 0.82$) and that of Carretta et al. (1999; M_V(HB) $= 0.18 \times$ [Fe/H] $+ 0.92$). The LDZ scale is at the basis of the DA90 calibration, whereas the Carretta et al. scale represents one of the most recent post-Hipparcos results. The coefficients of the interpolations are listed in Saviane et al. (1999). It is however important to stress that $d \sim 0.2$: since the RGB color is $(V-I)_0 > 0.8$ (cf. Fig. 1), then the denominator of Eq. (1) is significantly different from zero for any RGB star. Moreover, the r.m.s. scatter around the residuals is of the order of

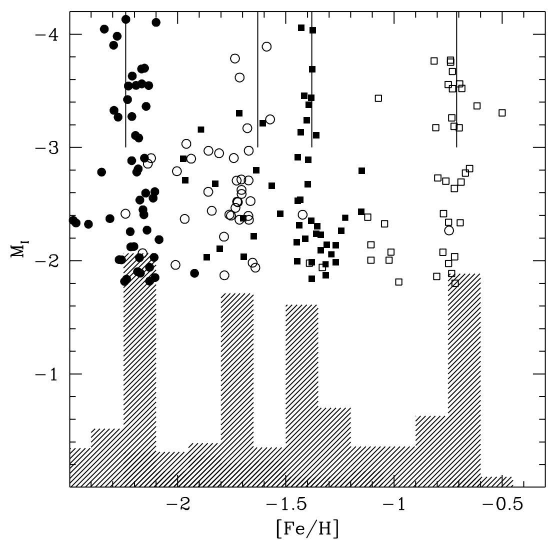

Figure 3: The RGBs of the clusters NGC 6341, NGC 6205, NGC 5904, and 47 Tuc, represented in the ([Fe/H], M_I) plane. The colors of the stars have been transformed into metallicities, using a quadratic relation derived from Eq. (1). The ZW84 metallicities of these clusters are −2.24, −1.63, −1.38, and −0.71, and are marked by vertical segments in the upper part of the figure. The [Fe/H] distributions of each RGB are represented by the histograms in the lower part of the figure

0.07 mag. The results of our fitting procedures are shown in Fig. 1, and one can see that the morphology-metallicity relation of the RGB is reproduced in a satisfactory way. The dashed curves represent the analytic function sampled at 0.1 dex steps, while the solid curves are the same function computed for the nominal metallicity of each cluser.

3 A Consistency Check

In order to test the analytic function, we used the set of metallicity indices that were measured on the 31 observed RGBs. Their trend with [Fe/H] was compared to the analytic one. Examples of these comparisons are shown in Fig. 2, where the indices $(V-I)_{-3.0}$ and $(V-I)_{-3.5}$ are plotted versus the GC97 and ZW84 metallicity scales. These indices, defined in DA90 and LFM93 respectively, are at the basis of [Fe/H] determinations in resolved galaxies of the LG, and represent the color of the RGB at an absolute magnitude $M_I = -3.0$ and -3.5. One can see that the trends predicted by the analytic function are in good agreement with the observed ones. In particular, for these two indices, the mean differences between the predicted and fitted indices are, on the ZW84 scale, around 0.03 dex and ~ 0.05 dex on the CG97 scale. For the ZW84 metallicity scale and the LDZ distance scale, our new calibrations were also compared to the relations obtained by DA90 and LFM93 (dashed lines in Fig. 2), and, again, the agreement was good. As further explained in Saviane et al. (1999), the observed differences are mainly due to a different choice for the fiducial 47 Tuc branch.

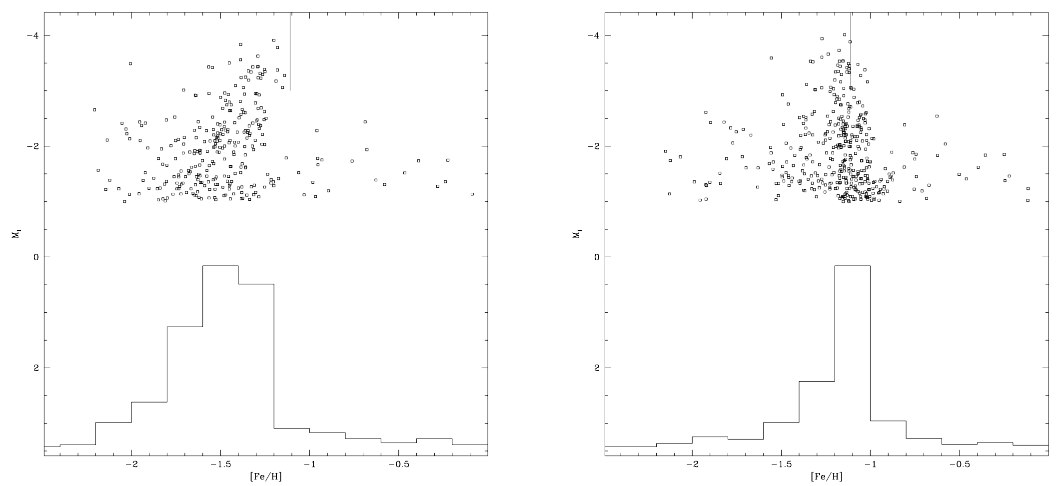

Figure 4: Same as Fig. 3, for the NGC 2808 giant branch (Bedin et al. 1999, in preparation). The left panel shows the [Fe/H] distribution (on the CG97 scale) obtained assuming $E_{B-V} = 0.23$, as in the updated Harris catalogue, while the right panel shows the result for $E_{B-V} = 0.15$. Only using the lower reddening value, is the nominal mean metallicity obtained ([Fe/H]=-1.11)

4 Application of the Analytic RGB: Some Test Cases

4.1 Metallicity Ranking of GGCs

Equation (1) can be written as a quadratic relation of [Fe/H] in terms of $(V-I)_0$ and M_I. Using this relation, one can therefore obtain the metallicity of *any RGB star*, provided that the distance and reddening of the star are known. An example of this is shown in Fig. 3, where the color of each star has been transformed into a metallicity. The RGBs of four of the clusters already used to define the grid, can therefore be represented in the ([Fe/H], M_I) plane (the ZW84 scale is used in this case). One can see that, as expected, the RGBs get linearized, since the points are now scattered around the mean metallicity of each cluster. The mean metallicity is also correctly recovered, within 0.1 dex.

This test suggests that one can hope to obtain both the reddening and the metallicity of a "typical" globular cluster, exploiting the fact that the *shape* of the RGB strongly depends on [Fe/H]. A first illustration that this could be the case, is now given.

4.2 The Reddening of NGC 2808

The reddening of NGC 2808 has been lately debated. The updated Harris (1996) catalog reports $E_{B-V} = 0.23$. However, according to Walker (1999), this value makes the shape of the cluster RGB incompatible with its metallicity. A lower reddening is suggested also in Sosin et al. (1997). We find confirmation of these claims if we look at Fig. 4, where the RGB of NGC 2808 has been transformed into the ([Fe/H], M_I) plane, for two values of the reddening. The photometric catalog has been taken from Bedin et al. (1999).

Both using the ZW84 metallicity and the GC97 one, it is found that a value $E_{B-V} \simeq 0.15$ allows us to recover the shape of the giant branch and the actual metallicity (right panel). On the contrary, the higher reddening value gets the RGB distorted (left panel).

The broader [Fe/H] distribution of NGC 2808, compared to that of the four clusters in

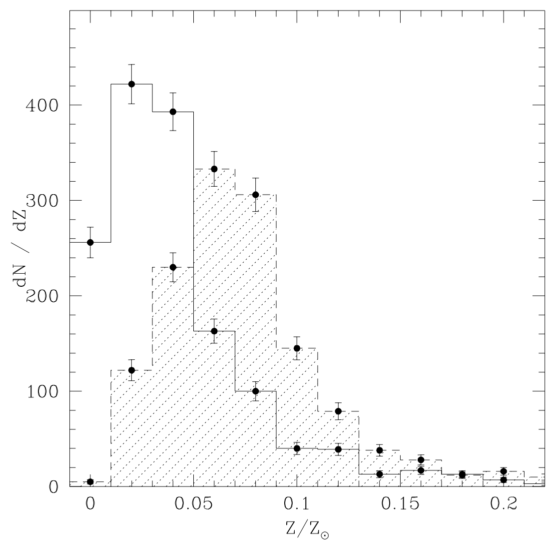

Figure 5: The metallicity distribution function obtained from the RGB stars of the Fornax dwarf spheroidal galaxy. The original photometry is that of Saviane, Held & Bertelli (1999). This figure has been obtained as Fig. 4, but absolute metallicity Z is used. The MDF obtained using the ZW84 scale is represented by the solid histogram, while that obtained using the CG97 scale is represented by the dashed and shaded histogram

Fig. 3, is probably due to the differential reddening that affects this cluster. In other words, there is no evidence for a real [Fe/H] dispersion. However, there are cases when a metallicity spread is expected, such as in composite systems. For example, positive [Fe/H] dispersions are indeed observed in many LG dwarf galaxies (see e.g. Mateo 1998 for a recent review). In these cases, the possibility to obtain a detailed metallicity distribution function (MDF), would be an important constraint to their star formation history (SFH).

An example of this can be found in Harris, Harris & Poole (1999; HHP99), where the MDF of the nearest giant elliptical galaxy, NGC 5128, is studied, and important clues to its formation are obtained. The availability of our new interpolation formulae should now make these studies more straightforward.

4.3 Chemical Enrichment in Local Group Dwarfs

In Fig. 5, we show the MDF obtained from the RGB of the Fornax dwarf spheroidal galaxy (Saviane, Held & Bertelli, 1999). After the color-metallicity relation has been applied, [Fe/H] has been transformed into the absolute metal mass fraction Z, so in the figure the number of stars as a function of $Z/Z_\odot$ is represented. This is an example of the application of our method to data for LG dwarfs (Held, Bertelli & Saviane, in preparation). The solid histogram shows the result when the ZW84 scale is adopted, while the result corresponding to the CG97 scale is plotted as a dashed shaded histogram.

No attempt has been made to correct the distribution for observational errors and biases, so we do not want to attach any quantitative conclusions to the plots. However, it is clear that they are significantly different. The distribution on the ZW84 scale resembles the outcome of an "instantaneous Simple model" of chemical enrichment (see e.g. Pagel, 1997, for a review), where a peak at $Z \sim 2\%$ solar is followed by an exponential decay, and a small fraction of stars more metal-poor than the peak is observed (see e.g. Fig. 12 of HHP99). On the other hand, the peak on the GC97 scale is located at a higher metallicity $Z \sim 7\%$ solar, and the number of stars more metal-poor than the peak is comparable to that of metal-rich ones. The interpretation of this distribution would be less straightforward. This difference is clearly due to the fact that in the CG97 scale the RGBs are more densely spaced towards lower metallicity than in the ZW84 scale (cf. Fig. 1). A given $(V - I)$ interval is then stretched into a larger [Fe/H] interval.

We then stress that the choice of a metallicity scale strongly affects our conclusions regarding the chemical enrichment of LG dwarf galaxies. A consensus should therefore be reached on one of the two scales.

Acknowledgements

Enrico V. Held and Luigi Bedin are thanked for the kind permission to use their data in the present study. Peter B. Stetson is aknowledged for suggestions that improved an early draft of this manuscript.

References

Carretta E., Gratton R., 1997, A&AS, 121, 95 (CG97)
Carretta E., Gratton R.G., Clementini G., Fusi Pecci F. 1999, ApJ, submitted, (astro-ph/9902086; C99)
Da Costa G.S., Armandroff T.E., 1990, AJ, 100, 162 (DA90)
Dean J.F., Warren P.R., Cousins A.W.J., 1978, MNRAS, 183, 569
Harris W.E., 1996, AJ, 112, 1487
Harris G.L.H., Harris W.E., Poole G.B., 1999, AJ, 117, 855 (HHP99)
Lee Y.W., Demarque P., Zinn R., 1990, ApJ, 350, 155 (LDZ)
Lee M.G., Freedman W.L., Madore B.F., 1993, ApJ, 417, 553 (LFM93)
Mateo M., 1998, ARA&A, 36, 435
Pagel B.E.J., 1997. *Nucleosynthesis and chemical evolution of galaxies*, Cambridge University Press, Cambridge, p. 218
Piotto G., Sosin C., King I.R., Djorgovski S.G., Rich R.M., Dorman B., Renzini A., Phinney S., Liebert J., 1997. In: R.T. Rood & A.Renzini (eds.) Advances in Stellar Evolution, Cambridge University Press, Cambridge, p. 84
Rosenberg A., Piotto G., Saviane I., Aparicio A., 1999a, A&AS, in press
Rosenberg A., Aparicio A., Saviane I., Piotto G., 1999b, A&AS, submitted
Rosenberg A., Saviane I., Piotto G., Aparicio A., 1999c, AJ, Nov. issue
Rutledge A.G., Hesser J.E., Stetson P.B., 1997, PASP, 109, 907 (RHS97)
Sandage A., Smith L.L., 1966, ApJ, 144, 886
Sandage A., Wallerstein G., 1960, ApJ, 131, 598
Saviane I., Held E.V., Piotto G., 1996, A&A, 315, 40
Saviane I., Rosenberg A., Piotto G., Aparicio A., 1999, A&A, in press
Saviane I., Held E.V., Bertelli G., 1999, A&A, in press
Sosin G., Dorman B., S. Djorgvski, Piotto G., Rich R.M., King I.R., Liebert J., Sterl E.P., Renzini A., 1997, ApJL, 480, 35
Walker A.R., 1999, AJ, 118, 432
Zinn R., West M., 1984, ApJS, 55, 45 (ZW84)